

# Evaluation of Optical Properties of Carbon Nano Structures Coating on Substrate Surface by Plasma Enhanced CVD

Zahra Khalaj, Mahmood Ghoranneviss, Shahriar Mirpour, Z.Ghorannevis

*Plasma Physics Research Center, Science and Research Branch, Islamic Azad University, Tehran, Iran,  
P.O.BOX:14665-678.*

*Author for correspondence: Prof. Mahmood Ghoranneviss*

*Tel: +98 21 44869624 Fax: +98 21 44869626 Email:Ghoranneviss@gmail.com*

The valence electron of carbon forms in different chemical bonds by means of three different hybridization: SP, SP<sup>2</sup> and SP<sup>3</sup> which leads to formation of various carbon nanostructures. The different types of carbon allotropes, especially diamond has a great influence on material's properties. In this work we investigated the growth of diamond-like carbons (DLC) on an aluminum and quartz substrate by DC plasma-enhanced chemical vapor deposition (DC-PECVD) system. The growth precursors consisted of methane diluted into hydrogen gas. The experiment was done in CVD reactor after the first pretreatment of the substrate using He, He-N<sub>2</sub> and He-O<sub>2</sub> gases in Plasma Jet system, separately and respectively. The results show the intensive changes on surface properties before and after deposition. The optical properties of the as-grown DLC structures were investigated. A possible growth scheme, based on qualitative analysis by scanning electron microscopy (SEM), Raman spectroscopy, Fourier transform infrared (FTIR) and UV-Visible-NIR, is presented in this paper.

**Key Words:** Plasma jet system, Diamond-like carbon, plasma etching, PECVD.

## 1.Introduction

Diamond-like carbon (DLC) films have been intensively studied for over two decades, owing to their excellent characteristics such as as low friction coefficient, wear resistance, chemical inertness, corrosion resistance, high hardness [1-4]. Because of its special properties it is used for different devices like FET and MEMS[5]. They are also used as solid lubricants, anti-reflection and protective coating on germanium, zinc-sulphide window, solar cells and bio-medical applications[5]. Generally, the most conventional constructions of DLC films are tetrahedrally bonded (sp<sup>3</sup>) and trigonally bonded (sp<sup>2</sup>) carbon atoms [6]. Some properties of diamond-like carbon such as high mechanical hardness, chemical and electrochemical inertness are related to tetrahedral bonding while electronic and optical properties are governed by trigonal bonding [7, 8]. There are several researches for DLC coating such as pulse laser deposition[9] (PLD), electron cyclotron resonance[10], sputtering[11], RF-assisted microwave[12], and plasma beam sources[13], plasma-enhanced chemical vapor deposition(PECVD) [14], etc. PECVD technique is one of the most suitable methods for producing DLC films. One of the most important advantages of the PECVD method is the possibility of deposition on a large area and at low temperature [6]. In this way a wide range of substrate material can be used. In most of the researches RF discharge was used to produce

DLC[15-19]. It is generally considered that DLC is not possible with DC-discharge due to deposition of dielectric films, the electrode exposed to the plasma gradually become covered with an insulator[5]. Therefore, although a DC discharge may be initiated, it will quickly extinguish as the electrons accumulate on the insulator and recombine with the available ions[5]. Using hydrogen dilution would do not let the target to cover with a hydrocarbon gas. In addition, DC-PECVD is suitable to use for DLC coating because of the low stress value in comparison with Rf-PECVD method [20].

In this work, we used DC-PECVD technique for growing diamond-like carbons on aluminum and quartz substrates. Two pretreatment steps were done to enhance the DLC growth. In the first step, the samples were etching treated in He, He-N<sub>2</sub> and He-H<sub>2</sub> separately and respectively by Plasma Jet system then loaded to PECVD and etched by methane. The mixture of CH<sub>4</sub>/H<sub>2</sub> was applied as a source and diluting gases for DLC growth. The characteristic of the samples were investigated by scanning electron microscopy (SEM), Raman spectroscopy, Fourier transform infrared (FTIR) and UV-Visible-NIR.

## 2.Experimental

### 2.1 Substrate pretreatment

Aluminum (99.99% purity) and quartz were used as substrates in this experiment for growing carbon nano structures. After cleaning the samples, they were pretreated by different type of etching gases in plasma jet system and were loaded to PECVD for deposition process.

The Plasma Jet system consists of a plasma needle which is the main part of the system. The plasma needle consists of a thin tungsten wire with sharp tip (diameter = 0.3 mm) as the central electrode insulated with a Pyrex tube (inner diameter = 1mm) which put into another Pyrex tube as the nozzle (inner diameter of 4.5 mm and length of 3 cm).

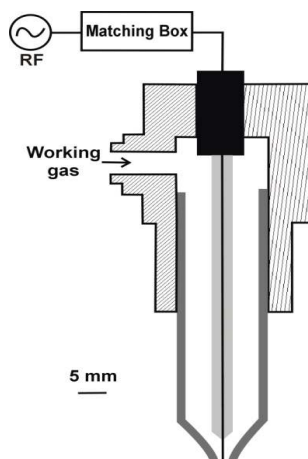


**Fig. 1** Schematic diagram of plasma jet system

The length of under exposure part of the metal wire of the glass insulator was 5 mm. The electrode was connected to a RF power supply antenna (13.56 MHz, Yarnikan Saleh Co). The forwarded power was about 70 Watt for all of the tests in this study. The working gas was 98

% pure helium because of the lowest breakdown voltage in atmospheric pressure property. The flow rate of filling gas was 1 lit/min which controlled by a flow-meter. This rate remained constant during all of the experiments. Moreover, 2% of pure Nitrogen ( $N_2$ ) and oxygen ( $O_2$ ) was injected as addition gas into some experiments. The samples with pure He, He- $N_2$  and He- $O_2$  treatments were named  $S_1, S_2, S_3$  for aluminum samples and  $S_4, S_5$  and  $S_6$  for quartz samples, separately and respectively. In the experiments the time for treatment and distance between electrode and sample is constant and 10 minute and 5 mm for all of the experiments, respectively. Figure 1 shows the schematic diagram of the plasma jet system.

## 2. CVD Growth Process

### 2.1. Plasma Etching

All the substrates were loaded to reaction chamber after pretreatments. The chamber was evacuated to  $3 \times 10^{-2}$  Torr before the etching gas was introduced into it. Using an etching gas before the main growth has a great influence on primary nucleation. The methane was introduced to the chamber as an etching gas in total pressure of 7 Torr. The samples were etching-treated in substrate temperature of  $190^\circ C$ . The duration of time for this experiment was 15 minutes.

### 2.3. Nucleation and Growth of the Diamond-like carbon

The diamond-like carbon structures were deposited on aluminum and quartz in DC-Plasma Enhanced Chemical Vapor Deposition (PECVD) system. Figure 2 shows the schematic diagram of the DC-PECVD system.

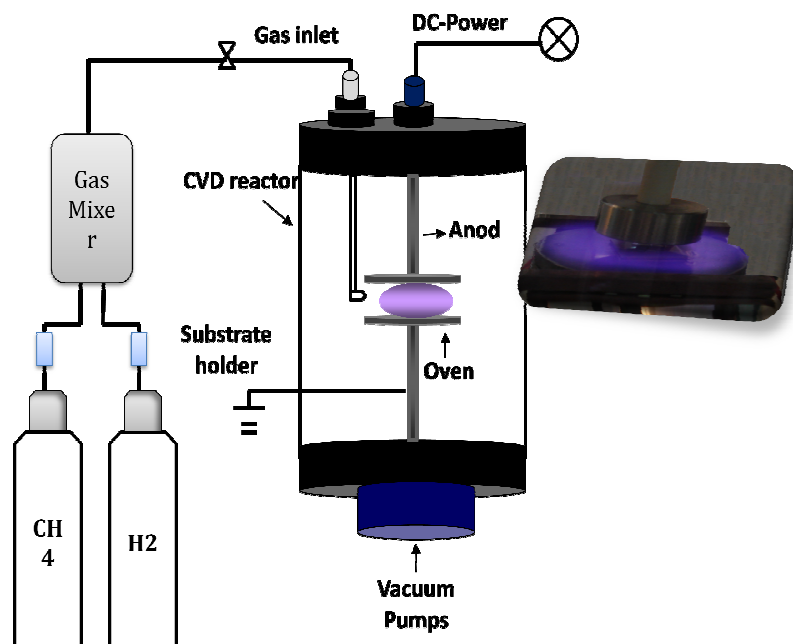


Fig.2 Schematic diagram of the PECVD system.

The central part of the DC-PECVD is a cylindrical process chamber with a diameter of 28cm consisting of a base and a cover. On the top of the system cover the DC source is flanged. The chamber can be opened for substrate handling by vertical shifting the aluminum cover on top.

After the chamber is pre-evacuated by rotary pump, the base pressure of the system is reached to  $\approx 10^{-2}$  Torr. The substrate is placed on a furnace right under the anode. The temperature of the substrates is monitored by a thermocouple. All the samples were grown in a mixture of methane and hydrogen (i.e. 10 vol. %  $\text{CH}_4/\text{H}_2$ ) and the operation gas pressure of 10 Torr. The duration of time was 75min, in which the temperature was  $300^\circ\text{C}$ . The main controllable growth parameters were applied voltage 450V, and plasma current was 30mA. After reaction, the samples were cooled down in vacuum. These conditions were fixed for all the samples studied here.

### 3. Results and Discussion

Raman spectroscopy is a non-destructive method for characterizing the quality and structural properties of carbon coating materials. Raman spectra of carbon materials such as diamond-like carbon structures show common features that indicates the crystalline graphite (G-peak) and disordered graphite (D-peak) peaks. The G peak attribution to stretching vibration mode of all pairs of  $\text{SP}^2$  sites in aromatic rings or  $\text{C}=\text{C}$  chains and D peak assigned to breathing mode of  $\text{SP}^2$  sites only in six-fold rings [21]. Fig. 3 shows a Raman spectrum of the DLC samples measured by the second harmonic of a Nd:YLF laser with an excitation wavelength of 532 nm. As we can see in Fig. 3(a), there are two peaks at 1375 and 1575.37 which related to D and G band respectively. Whereas the D band and G band are 1463 and 1527.13 for sample  $S_2$  and there are 1409 and 1575.19 for sample  $S_3$  which confirm the DLC deposition in substrate surface (See Fig. 3(b,c)). The intensity of D peak and G peak,  $I(\text{D})/I(\text{G})$ , and the position of the G peak,  $\text{pos}(\text{G})$ , provides information about qualitative assessment of amount of  $\text{SP}^3$  in diamond-like carbon films[21].

We observed that ratio  $I(\text{D})/I(\text{G})$  for the DLCs grown on Al substrate. The results show that the plasma etching treatment of DLC films by plasma jet system leads to the shift of the two peaks towards lower wave numbers and a decrease in the  $I(\text{D})/I(\text{G})$  ratio.

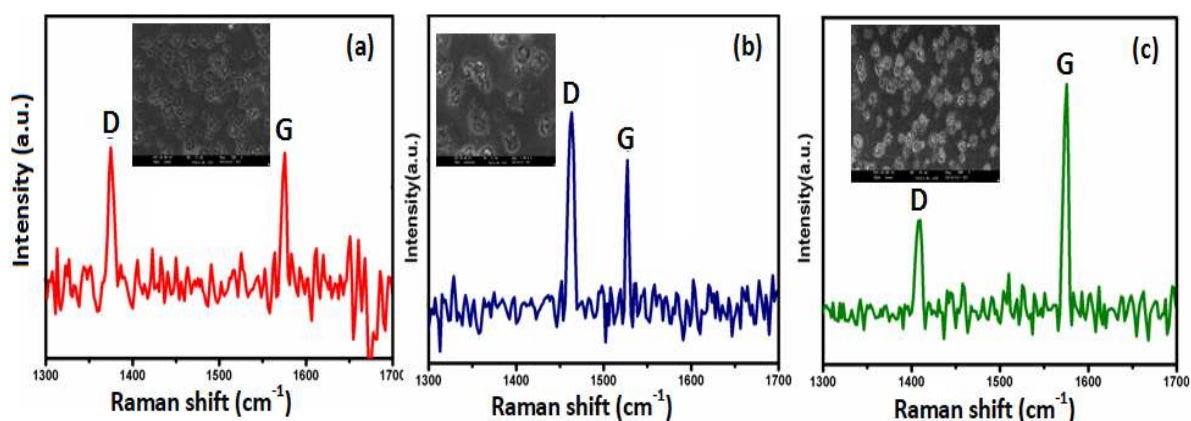


**Fig. 3** Raman spectra of coated surface of PECVD DLC film and the corresponding SEM images;(a)  $S_1$ , (b)  $S_2$ , (c)  $S_3$

As  $SP^3$  content increases in DLC structures, the G peak position shift toward lower wave numbers and the intensity ratio of the I(D)/I(G) decreases [21]. Due to the spectra of the samples the I(D)/I(G) ratio is decreased from  $S_2$  to  $S_1$  and  $S_3$  respectively. The results show that, the quality of the DLC grown on Al increased by decreasing the ratio of I(D)/I(G). Therefore, the DLCs deposited on Al substrates ( $S_3$ ) which plasma etching-treatment done by He- $O_2$  gases has more  $SP^3$  bonds and their quality are better than the others. It could be mentioned that the  $O_2$  plasma produces energetic oxygen species, which can be reacted easily to the aluminum surface. Also, the average roughness of the surface is change by etching treatment process. Etching the substrate surface before CVD growth creates the suitable sites for trapping carbon atoms after ionization in CVD reactor. This leads to the first nucleation of the DLC structures. In addition, the more reactive surface that etching treated by plasma jet system with He- $O_2$  leads to creation of the most suitable surface in comparison with He- $N_2$  and pure He. The results of the I(D)/I(G) confirms this idea (See Table 1).

**Table 1.** Raman study for DLC synthesized on aluminum substrates.

Sample	Plasma jet treatments	Plasma CVD treatments	D-Peak( $cm^{-1}$ )	G-Peak( $cm^{-1}$ )	I(D)/I(G)
Al	He	$CH_4$	1375	1575.37	1.05
Al	He- $N_2$	$CH_4$	1463	1527.13	1.27
Al	He- $O_2$	$CH_4$	1409	1575.19	0.46

The surface morphology of the DLCs was shown in Fig.3. As we can see, diamond-like carbons grown on  $S_3$  and  $S_1$  are more condense in comparison with  $S_2$  which confirms the Raman spectroscopy analysis.

FTIR is another widely used technique to characterize the bonding in DLC [5]. It is used to determine the chemical group constituting the films [5]. Figure 4 shows the FTIR spectrum of the DLCs deposited on aluminum substrates, which pretreated by He, He- $N_2$  and He- $O_2$ , respectively. The FTIR spectrum consists of bending and stretching vibration modes of C-H groups. There are observed regions of C-H bending and stretching modes at 1300–1700  $cm^{-1}$  and 2700–3100  $cm^{-1}$ , respectively [21,22]. The infrared spectra of DLCs deposited on  $S_1$ ,  $S_2$  and  $S_3$  substrates (Fig. 4) shows peaks at around 1450  $cm^{-1}$  which are associated with C-H<sub>2</sub> vibration modes having  $SP^2$  and  $SP^3$  hybridization carbon atoms in DLCs, respectively. The broad absorption peak at 2861  $cm^{-1}$  is in agreement with other literatures [22,23] and can be attributed to  $SP^3$  bonded  $CH_x$  ( $x = 1, 2, 3$ ) in soft and hard diamond-like carbon films[21]. The other peak observed at around 2969  $cm^{-1}$  corresponds to  $SP^3$   $CH_3$  configuration in soft diamond-like carbon structure. This spectra is shown a peak at 2969  $cm^{-1}$  which is assigned to the  $SP^3$   $CH_3$  in soft DLC. The other peak which is also observed at around 910  $cm^{-1}$  could be due to the existence of  $SP^2$   $CH_2$  which is attributed to the soft and hard DLC. In addition, there is a  $SP^3$  bonded in  $CH_2$  in soft and hard DLC in 2923 $cm^{-1}$ , which observed in all samples, and also  $SP^3$  CH in hard DLC.

**Table 2.** FTIR results for DLC grown on Al substrate, pretreated by different etching gases.

<b>Sample</b>	<b>Wavenumber(<math>\text{cm}^{-1}</math>)</b>	<b>Assignment</b>
<b>S<sub>1</sub></b>	755	<i>Arom.</i> $\text{SP}^2$ CH
	910	<i>Olef.</i> $\text{SP}^2$ $\text{CH}_2$
	1450	<i>Olef.</i> $\text{SP}^2$ $\text{CH}_2$ , $\text{SP}^3$ $\text{CH}_2$
	2861	$\text{SP}^3$ CH, $\text{SP}^3$ $\text{CH}_2$ , $\text{SP}^3$ $\text{CH}_3$
	2923	$\text{SP}^3$ $\text{CH}_2$ , $\text{SP}^3$ CH
	2969	$\text{SP}^3$ $\text{CH}_3$
	3299	SP CH
<b>S<sub>2</sub></b>	756	<i>Arom.</i> $\text{SP}^2$ CH
	910	<i>Olef.</i> $\text{SP}^2$ $\text{CH}_2$
	1450	$\text{SP}^2$ $\text{CH}_2$ , $\text{SP}^3$ $\text{CH}_2$
	2861	$\text{SP}^3$ (CH, $\text{CH}_2$ , $\text{CH}_3$ )
	2923	$\text{SP}^3$ $\text{CH}_2$ , $\text{SP}^3$ CH
	2969	$\text{SP}^3$ $\text{CH}_3$
	3300	SP CH
<b>S<sub>3</sub></b>	910	<i>Olef.</i> $\text{SP}^2$ $\text{CH}_2$
	1450	<i>Olef.</i> $\text{SP}^2$ $\text{CH}_2$ , $\text{SP}^3$ $\text{CH}_2$
	2861	$\text{SP}^3$ CH, $\text{SP}^3$ $\text{CH}_2$ , $\text{SP}^3$ $\text{CH}_3$
	2923	$\text{SP}^3$ $\text{CH}_2$ , $\text{SP}^3$ CH
	2969	$\text{SP}^3$ $\text{CH}_3$

In Table 2 various peaks, their corresponding wave numbers and their assignment to different bandings of each sample are brought out which are come from the Fourier transform infrared spectra of those DLCs. The present FTIR studies confirms previous findings and contributes [21,24].

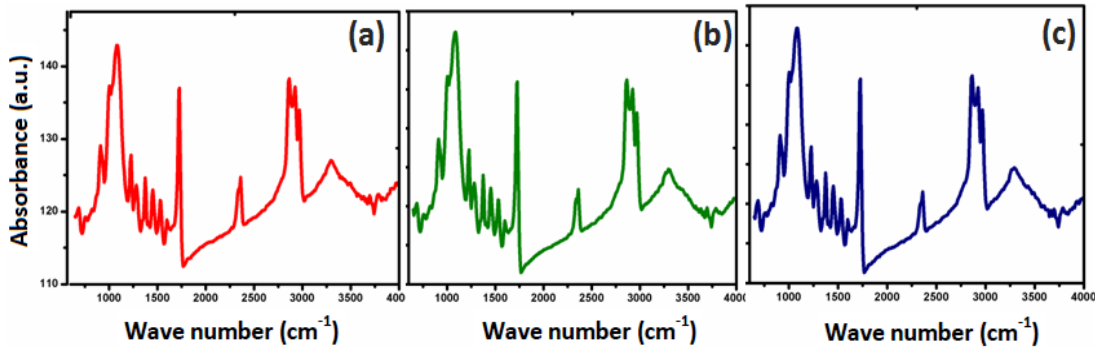


**Fig. 4** FTIR spectra of the DLC grown on Al substrates: (a) S<sub>1</sub>, (b) S<sub>2</sub>, (c) S<sub>3</sub>.

The transmittance for S<sub>4</sub>, S<sub>5</sub> and S<sub>6</sub> which pretreated in He, He-O<sub>2</sub> and He-N<sub>2</sub> were shown in Fig.5 (a-d). Figure 5(a) shows the UV transmission spectra of the diamond-like carbon grown on quartz substrates. The transmittance varied within the wavenumber from ~30% near 240 $\text{cm}^{-1}$  to ~90% near 2500  $\text{cm}^{-1}$ . The pattern shows that there is slope within the ~400 $\text{cm}^{-1}$ -

650 $\text{cm}^{-1}$  from 78% to 75% and a sharp increase in transmittance make appear in 650 $\text{cm}^{-1}$  to 900 $\text{cm}^{-1}$  (~ 74% to 85%). There is no tangible change in the transmission in ~900  $\text{cm}^{-1}$  to ~2250  $\text{cm}^{-1}$  and the average transmittance was near 85% in S<sub>4</sub>. Figure 5 (b) and (c) show the transmittance for S<sub>5</sub> and S<sub>6</sub> respectively. Figure 5(b) shows the average transmission near 19%, but it increased at larger wavenumber to 85%. By changing the plasma jet treatment's gas from He to He-O<sub>2</sub>, we can see a remarkable change from 450-700 $\text{cm}^{-1}$ . There is an intensive changes in 240-750  $\text{cm}^{-1}$  from 70% to 80%. The slope of the pattern is constant and does not change in 750 $\text{cm}^{-1}$  to 2500 $\text{cm}^{-1}$ . Also there is a change from He-O<sub>2</sub> to He-N<sub>2</sub> in optical properties of the DLC grown on surface. The result of the S<sub>4</sub> and S<sub>6</sub> for He and He-N<sub>2</sub> treatments are close to each other. The oxygen is a reactive gas and make the surface suitable for DLC growth. However, this is not seen for He and He-N<sub>2</sub> in comparison with He-O<sub>2</sub>.

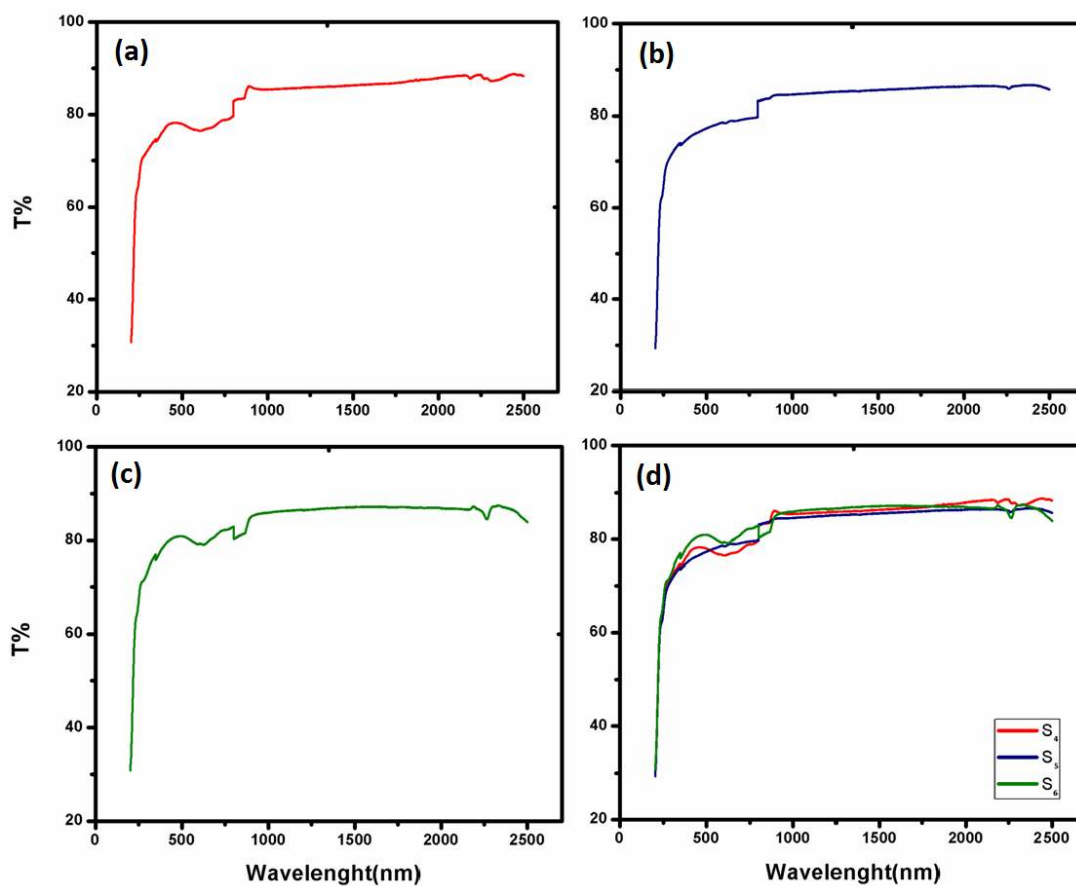


**Fig.5** The UV-Vis transmission Spectra of DLC grown on quartz: (a) S<sub>4</sub>, (b) S<sub>5</sub>, (c) S<sub>6</sub>, (d) comparison.

Figure 6 show the Reflection pattern for S<sub>4</sub>, S<sub>5</sub> and S<sub>6</sub> respectively. As the figure shows there reflection spectrum of S<sub>4</sub> and S<sub>5</sub> are nearly same. However the average reflectance for these samples was near 7.5% and 6% respectively. The results show that there is no slope in 1500-2500 $\text{cm}^{-1}$  for both samples and the average reflectance was near 7% for both of them. It is also noticed that as figure 6(d) indicates, there are slope within the non thermal radiation (700-1100 $\text{cm}^{-1}$ ) is higher than the thermal radiation range (1100-2500 $\text{cm}^{-1}$ ) for all samples.

Due to the investigations, oxygen atoms indeed played an important role. The results indicate that the sufficient emission intensities of important chemical species such as atomic oxygen, CO, CH [25] in plasma under low temperature conditions make the surface suitable for hydrocarbon bonding and had a beneficial effect on DLC growth.

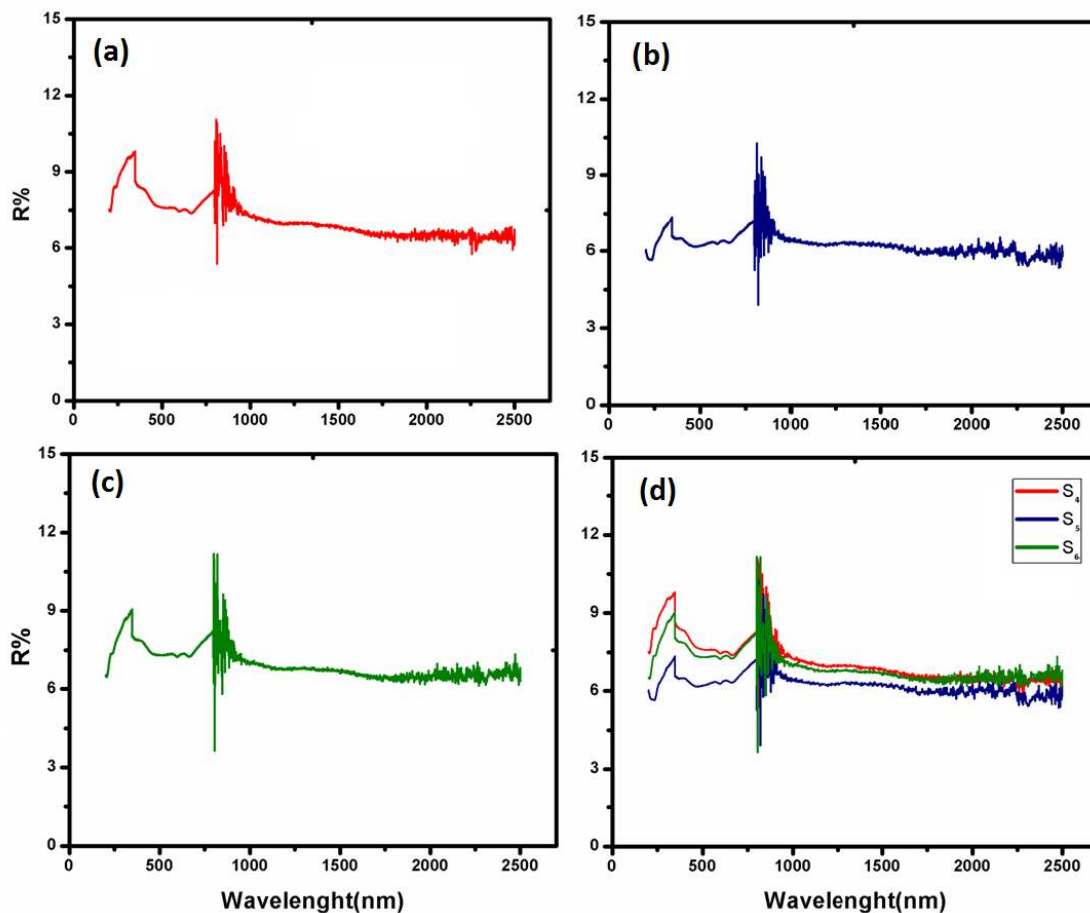


**Fig.5** The Reflection Spectra of DLC grown on quartz: (a) S<sub>4</sub>, (b) S<sub>5</sub>, (c) S<sub>6</sub>, (d) comparison.

## Conclusion

Diamond-like carbons were deposited on aluminum and quartz by DC-PECVD method in a mixture of methane and hydrogen. The samples were pretreated in two steps using He, He-N<sub>2</sub>, He-O<sub>2</sub> and CH<sub>4</sub> by plasma jet and PECVD methods separately. Due to the Raman and FTIR results, the optimum condition was obtained in a case of using He-O<sub>2</sub> for surface pretreatment. Due to the investigations, oxygen atoms indeed played an important role. The results indicate that the sufficient emission intensities of important chemical species such as atomic oxygen, in plasma jet system under low temperature conditions make the surface suitable for hydrocarbon bonding and had a beneficial effect on DLC growth.



## References

- [1] M. Azzi, P. Amirault, M. Paquette, J.E. Klemberg-Sapieha, L. Martinu, *J. Surface & Coatings Technology* 204 (2010) 3986–3994.
- [2] P.D. Maguire, J.A. McLaughlin, T.I.T. Okpalugo, P. Lemoine, P. Papakonstantinu, E.T. McAdams, M. Needham, A.A. Ogwu, M. Ball, G.A. Abbas, *Diamond Relat. Mater.* 14 (2005) 1277.
- [3] J. Robertson, *Mater. Sci. Eng. R* 37 (2002) 129.
- [4] Deok Yong Yun, Won Seok Choi, Yong Seob Park, Byungyou Hong, *Applied Surface Science* 254 (2008) 7925–7928.
- [5] Rishi Sharma, P.K. Barhai, Neelam Kumari, *Thin Solid Films* 516 (2008) 5397–5403.
- [6] S.I. Hosseini, B. Shokri, M. Abbasi Firouzjah, S. Kooshki, M. Sharifian, *Thin Solid Films* 519, (2011) 3090–3094.
- [7] K. Wang, H. Liang, J. Martin, T. Le Mogne, *Appl. Phys. Lett.* 91 (2007) 051918.
- [8] R. Paul, S. Das, S. Dalui, R. Gayen, R. Roy, R. Bhar, A. Pal, *J. Phys. D Appl. Phys.* 41 (2008) 055309.
- [9] A.A. Voennodin, M.S. Donley, *Surf. Coat. Tech.* 82, (1996) 199.
- [10] P. Reinke, W. Jacob, W. Möller, *J. Appl. Phys.* 74 (1993) 1354.
- [11] K. Bewilogua, R. Wittorf, H. Thomsen, M. Weber, *Thin Solid Films* 447, (2008) 142.
- [12] J.E. Bourée, C. Godet, B. Dre'villon, R. Etemadi, T. Heitz, J. Cernogora, J.L. Fave, *J. Non-Cryst. Solids* 198–200 (1996) 623.
- [13] M. Weiler, S. Sattel, T. Giessen, K. Jung, H. Erhardt, V.S. Veerasamy, J. Robertson, *Phys. Rev. B* 53 (1993) 1594.
- [14] A.A. Ogwu, R.W. Lambertson, P.D. Maguire, J.A. McLaughlin, *J. Phys. D-App. Phys.* 32, (1999) 981.
- [15] S. Aisenberg, R. Chabot, *J. Appl. Phys.* 42 (1971) 2953.
- [16] D.S. Whitmell, R. Williamson, *Thin Solid Films* 35 (1976) 253.
- [17] A. Bubenzer, B. Dischler, G. Brandt, P. Koidl, *J. Appl. Phys.* 54 (8) (1983) 4590.
- [18] A. Dhawan, S. Roy Chowdhuri, P.K. De, S.K. Sharma, *Bull. Mater. Sci.* 26 (6) (2003) 609.
- [19] Ying Li, Li Qu, Fuihui Wang, *Corros. Sci.* 45 (2003) 1367.
- [20] A. Grill, V. Patel, *Diamond Relat. Mater.* 2, (1993) 1519.
- [21] Elnaz Vaghri, Zahra Khalaj, Mahmood Ghoranneviss, Majid Borghei, *J. Fusion Energy*, xxx (2011) xxx.
- [22] G.E. Stan, D.A. Marcov, A.C. Popa, M.A. Husanu, *Nanomaterials. Biostructures.* 5, (2010) 705–718.
- [23] D.Y. Yun, W.S. Choi, Y.S. Park, B. Hong, *Appl. Surf. Sci.* 254, (2008) 7925–7928.
- [24] J. Robertson, *Prog. Solid. State. Ch.* 21, (1991) 199.
- [25] Chia-Fu Chen, Sheng-Hsiung Chen, Tsao-Ming Hong, Jen-Shiang Leu, *Thin Solid Films*, 253 (1994) 162-167.